# Prelaunch Calibration of the Advanced Microwave Sounding Unit-A for NOAA-K

Tsan Mo

***Abstract*—The thermal-vacuum chamber calibration data from the advanced microwave sounding unit-A (AMSU-A) for NOAA-K, which will be launched in 1997, were analyzed to evaluate the instrument performance, including calibration accuracy, nonlinearity, and temperature sensitivity. Particularly, the nonlinearity parameters which will be used for correcting the nonlinear contributions from an imperfect square-law detector were determined from this data analysis. It was found that the calibration accuracies (differences between the measured scene radiances and those calculated from a linear two-point calibration formula) are polarization-dependent. Channels with vertical polarizations show little cold biases at the lowest scene target temperature 84 K, while those with horizontal polarizations all have appreciable cold biases, which can be up to 0.6 K. It is unknown where these polarization-dependent cold biases originate, but the instrument's manufacturer suggests that the source of the observed biases is probably due to some low-level coherent radiation leakage from the instrument itself. The existence and magnitude of nonlinearities in each channel were established and a quadratic formula for modeling these nonlinear contributions was developed. The model was characterized by a single parameter $u$, values of which were obtained for each channel via least-squares fit to the data. Using the best-fit $u$ values, we performed a series of simulations of the quadratic corrections which would be expected from the space data after the launch of AMSU-A on NOAA-K. In these simulations, the cosmic background temperature of 2.73 K (instead of 84 K that was used in the thermal-vacuum chamber test) was adopted as one of the two reference points of calibration. The largest simulated nonlinear correction is about 0.3 K, which occurs at channel 15 when the instrument temperature is at 38°C. Others are less than 0.2 K in the remaining channels.**

## I. Introduction

AMSU-A, which is a new generation of total-power microwave radiometers, consists of 15 channels in two separate units: AMSU-A2 with two channels at 23.8 and 31.4 GHz; and AMSU-A1 with 12 channels in the range of 50.3 to 57.290344 GHz plus one channel at 89.0 GHz. Totally, AMSU-A1 furnishes 13 channels (channels 3 through 15) using two antenna systems, A1-1 and A1-2. The 12 oxygen-band channels (channels 3–14) will provide the microwave temperature sounding for regions from the Earth's near-surface to about 42 kilometer (km), or from 1000 to 2 millibars (mb). Channels 3 and 4 can also provide surface emissivity information. The remaining three channels (channels 1, 2, and 15) will aid the temperature sounding by correcting for the surface emissivity, atmospheric liquid water, and total precipitable water. These window channels also provide information on precipitation, sea ice, and snow coverage. Each of the AMSU-A antenna systems is required to have a nominal field-of-view (FOV) 3.3° at the half-power points and to cover a crosstrack scan of ±48°20′ (to beam centers) from the nadir direction with 30 Earth FOV's per scan line. Beam positions 1 and 30 are the extreme scan positions of the Earth views, while beam positions 15 and 16 are near the nadir direction. Onboard blackbody and cold space calibrations will be performed once every eight seconds for each scan line.

Three AMSU-A flight models, i.e., protoflight model (PFM), flight model 1 (FM1) and flight model 2 (FM2) have been built by GenCorp/Aerojet Electronic Systems Division, the main AMSU-A contractor, who is building two additional flight models. These AMSU-A instruments will be flown aboard the NOAA-K, L, M, N, and N spacecrafts, which constitute a new generation of polar-orbiting operational environmental satellites (POES). The first AMSU-A instrument is scheduled for launch in 1997 on NOAA-K, which will be renamed as NOAA-15 after launch. This follows the tradition that a NOAA spacecraft is named by an alphabetical letter before launch after which, a numerical series number replaces its letter nomenclature. The AMSU-A on NOAA-K consists of AMSU-A2 PFM and AMSU-A1 FM1, both of which passed the specification tests first.

Each of the flight models were tested and calibrated in a thermal-vacuum (T/V) chamber by its manufacturer. NOAA scientists analyze and evaluate these test data to determine the instrument's radiometric characteristics which will aid the development of the operational calibration algorithm for processing the in-orbit AMSU-A data. Particularly, the nonlinearity parameters which will be used in the AMSU-A calibration algorithm for correcting the nonlinear contributions from an imperfect square-law detector must be extracted from the prelaunch calibration data.

This study was undertaken to analyze and evaluate the T/V chamber test data from the first set of AMSU-A instruments to be launched aboard NOAA-K. We also developed an analytic formula that can simulate quantitatively the magnitude of the nonlinearity contributions to the retrieved brightness temperatures between 2.73 and 300 K from the postlaunch data. The results presented in this study explain how the new AMSU-A data will be processed.

In the following sections, we present the results of our data analysis. Specification topics evaluated in this analysis include calibration accuracy, nonlinearity, and radiometric temperature

Manuscript received December 4, 1995; revised April 19, 1996.
The author is with NOAA/NESDIS, Office of Research and Applications, Satellite Research Laboratory, Washington, DC 20233 USA.
Publisher Item Identifier S 0018-9480(96)05637-2.

TABLE I
NUMBER OF PRT'S IN EACH CALIBRATION TARGET AND CHANNELS PROVIDED BY INDIVIDUAL ANTENNA SYSTEMS THE LAST ROW GIVES THE NUMBER OF SCANS COLLECTED IN THE CALIBRATION FOR EACH SYSTEM

| Items | AMSU Antenna Systems | | | Remarks |
|---|---|---|---|---|
| | A2 | A1-2 | A1-1 | |
| PRTs in Warm Target | 7 | 5 | 5 | |
| PRTs in Cold Target | 11 | 7 | 7 | |
| PRTs in Scene Target | 11 | 7 | 7 | |
| Channels | 1 & 2 | 3, 4, 5 & 8 | 6, 7, & 9-15 | |
| PLLO#2 | - | - | Ch. 9-14 | Backup PLLO |
| N(Scan NO.) | 120 | 400 to 900 | 400 to 900 | See Note 1 |

Note: 1. For A1-1 & A1-2: N=400, 400, 550, 725, 725, and 900 when the scene target temperature $T_s$=84, 130, 180, 230, 280, and 330K, respectively.

TABLE II
UNCERTAINTIES IN BRIGHTNESS TEMPERATURE AND MEASUREMENT ERRORS

| Origin of Errors | AMSU-A2 | | AMSU-A1 | |
|---|---|---|---|---|
| | Bias (K) | Random (K) | Bias (K) | Random (K) |
| Warm Target | -0.050 | ±0.122 | -0.050 | ±0.122 |
| Cold Target | 0.024 | ±0.105 | 0.024 | ±0.091 |
| Scene Target | 0.002 | ±0.101 | 0.002 | ±0.090 |

sensitivity (or NE$\Delta$T, the noise-equivalent temperature). Section I gives an introduction and Section II presents a brief description of the T/V chamber test data. The calibration algorithm is described in Section III and results are presented in Section IV. Conclusion and discussion are given in Section V.

## II. DESCRIPTION OF DATA

The description of the AMSU-A hardware configuration has been given elsewhere [1], [2] and a brief functional description of the AMSU-A system is given in Appendix A. In this study, we mainly present the calibration process and algorithm for converting radiometric counts into brightness radiances (or temperatures). All data used in this report were taken by Aerojet in its T/V test chamber using the full scan mode. In this mode, AMSU-A scans through 30 scene-view (or beam) positions, the cold "space target," and the warm internal blackbody target once every eight seconds. It takes one look (or sample) at each scene position and two looks at the cold and warm targets, respectively. In the T/V chamber, the space target was simulated by a blackbody target maintained at 84 K, which is higher than the cosmic background temperature of 2.73 K that will be employed in real space data. Therefore, the nonliearity corrections in space can only be simulated, using the parameters extracted from the test data. The temperature of the internal blackbody target varies passively with the instrument temperature that is defined as the temperature measured by the RF Shelf sensor in each antenna system. The scene calibration target was fixed at beam position 6 (31°40′ from nadir). Each antenna system looks at its own individual cold, warm, and scene targets, temperatures of which are measured by Platinum Resistance Thermometers (PRT's). The numbers of PRT's used to measure the physical temperatures of the scene, cold, and warm calibration targets in each antenna system are given in Table I, which also lists the channels provided by each AMSU-A antenna system. Channels 9–14 have both primary and secondary phase locked loop oscillators (called PLLO#1 and PLLO#2, respectively) built-in. The PLLO#2 will be used for backup if the PLLO#1 fails. Invar high-$Q$ cavity stabilized local oscillators [2] are used in other channels.

The physical temperatures of scene and cold targets measured by individual PRT's were provided in Kelvin (K) on Aerojet's data tape. However, the signals from the PRT's monitoring the warm internal blackbody targets are given in counts, which must be converted to PRT temperatures. The normal approach of deriving the PRT temperatures from counts is a two-step process: (1) the resistance of each PRT in ohms is computed by a count-to-resistance look-up table provided by the manufacturer, and (2) the individual PRT temperature in degrees Celsius is obtained from an analytic PRT equation [3]. However, the two steps can be compressed to a single step with negligible errors. Appendix B gives a description of the process. This single step process, which will be used in operation, computes the PRT temperatures directly from the PRT counts, using a cubic polynomial

$$T_k = \sum_{j=0}^{3} f_{kj} C_k^j \tag{1}$$

where $T_k$ and $C_k$ represent the temperature and count of the PRT $k$. The polynomial coefficients, $f_{kj}$, are obtained from least-square fit for each PRT at NOAA. Equation (1) also applies to 47 other housekeeping temperature sensors, such as the mixers, the IF amplifiers and the local oscillators. All these polynomial coefficients will be stored in the Header of AMSU-A Level 1b data and its format [4] can be downloaded via the Internet.

The mean internal blackbody temperature, $T_w$, is calculated from the individual PRT temperatures

$$T_w = \frac{\sum_{k=1}^{m} w_k T_k}{\sum_{k=1}^{m} w_k} + \Delta T_w \tag{2}$$

where $m$ represents the number of PRT's for each antenna system (as listed in Table I) and $w_k$ is a weight assigned to each PRT. The quantity $\Delta T_w$, which corrects any warm target bias, has been described in [5]. The $\Delta T_w$ values were obtained by setting the temperature of scene target equal to that of the internal blackbody target. Using the temperatures of the scene and cold targets as the two reference points, one can compute the radiometric temperature $T_{w\text{rad}}$ of the internal blackbody target from the two-point calibration formula (as defined in Section III). The $\Delta T_w$ is defined as the difference of $T_{w\text{rad}}$ and

TABLE III
CHANNEL CHARACTERISTICS AND SPECIFICATIONS OF AMSU-A2 PFM AND AMSU-A1 FM1 FOR NOAA-K

| Channel Number | Channel Frequency (MHz) Specification | Measured * | No. of Bands | Measured 3-dB Bandwidth (MHz) | NEΔT (K) Spec. | Measred | Beam # Efficiency | Polarization (NADIR) | FOV** (deg.) | Remarks |
|---|---|---|---|---|---|---|---|---|---|---|
| 1 | 23800 | 23800.37 | 1 | 251.02 | 0.30 | 0.211 | 95% | V | 3.52 | A2/PFM |
| 2 | 31400 | 31400.42 | 1 | 161.20 | 0.30 | 0.265 | 97% | V | 3.40 | " |
| 3 | 50300 | 50299.91 | 1 | 161.14 | 0.40 | 0.219 | 95% | V | 3.75 | A1/FM1 |
| 4 | 52800 | 52799.39 | 1 | 380.52 | 0.25 | 0.143 | 95% | V | 3.72 | " |
| 5 | 53596 ± 115 | 53595.41 ± 115 | 2 | 168.20 I 168.20 | 0.25 | 0.148 | 95% | H | 3.69 | " |
| 6 | 54400 | 54399.53 | 1 | 380.54 | 0.25 | 0.154 | 95% | H | 3.68 | " |
| 7 | 54940 | 54940.64 | 1 | 380.56 | 0.25 | 0.132 | 95% | V | 3.61 | " |
| 8 | 55500 | 55498.70 | 1 | 310.34 | 0.25 | 0.141 | 96% | H | 3.62 | " |
| 9 | fo = 57290.344 | fo = 57290.33 | 1 | 310.42 | 0.25 | 0.236 | 96% | H | 3.51 | " |
| 10 | fo ± 217 | fo ± 217 | 2 | 76.58 I 76.58 | 0.40 | 0.250 | | H | " | " |
| 11 | fo ± 322.2 ± 48 | fo ± 322.2 ± 48 | 4 | 34.28 / 35.11 I 35.11 / 34.28 | 0.40 | 0.280 | | H | " | " |
| 12 | fo ± 322.2 ± 22 | fo ± 322.2 ± 22 | 4 | 15.08 / 15.29 I 15.29 / 15.08 | 0.60 | 0.400 | | H | " | " |
| 13 | fo ± 322.2 ± 10 | fo ± 322.2 ± 10 | 4 | 7.92 / 7.93 I 7.93 / 7.92 | 0.80 | 0.539 | | H | " | " |
| 14 | fo ± 322.2 ± 4.5 | fo ± 322.2 ± 4.5 | 4 | 2.94 / 2.92 I 2.92 / 2.94 | 1.20 | 0.914 | | H | " | " |
| 15 | 89000 | 88997.00 | 1 | 1998.98 | 0.50 | 0.166 | 98% | V | 3.80 | " |

* At temperature 18 degree C. ** Specification is required to have 3.3 degrees ± 10% for all channels. # Measured.

TABLE IV
VALUES OF THE NONLINEARITY PARAMETER $u$ OBTAINED FROM LEAST-SQUARES FIT TO DATA AT THREE INTRUMENT TEMPERATURES. THE $u$ HAS A DIMENSION OF $(\mathrm{m}^2\text{-sr-cm}^{-1})/\mathrm{mW}$

**AMSU-A2 Channels:** / **AMSU-A1-2 Channels:**

| Instrument Temperature (C) | CH. 1 | CH. 2 | Instrument Temperature (C) | CH. 3 | CH. 4 | CH. 5 | CH. 8 |
|---|---|---|---|---|---|---|---|
| 29.7 | 1.109810 | -0.050246 | 38.76 | 0.048428 | 0.269246 | -0.013142 | -0.009438 |
| 11.5 | 1.128380 | 0.309354 | 18.03 | 0.080626 | 0.439102 | -0.003414 | 0.001171 |
| -6.6 | 0.980173 | -0.072332 | -2.59 | 0.055511 | 0.444932 | -0.027906 | -0.000369 |

**AMSU-A1-1 Channels: (PLLO #1)**

| Instrument Temperature (C) | CH. 6 | CH. 7 | CH. 9 | CH. 10 | CH. 11 | CH. 12 | CH. 13 | CH. 14 | CH. 15 |
|---|---|---|---|---|---|---|---|---|---|
| 38.09 | 0.232594 | 0.112400 | -0.022126 | -0.029466 | 0.220561 | 0.139549 | 0.044524 | 0.021492 | 0.188672 |
| 18.03 | 0.087373 | -0.015400 | -0.047238 | -0.169687 | 0.020415 | -0.025818 | -0.284480 | -0.022299 | 0.103593 |
| -2.61 | -0.010790 | -0.000626 | -0.148429 | -0.239106 | 0.075740 | -0.082410 | -0.353876 | -0.371479 | 0.092549 |

**AMSU-A1-1 Channels: (PLLO #2)**

| Instrument Temperature (C) | CH. 9 | CH. 10 | CH. 11 | CH. 12 | CH. 13 | CH. 14 |
|---|---|---|---|---|---|---|
| 38.77 | 0.049806 | 0.016424 | 0.174105 | 0.035468 | 0.001316 | -0.063196 |
| 16.95 | -0.085951 | -0.130501 | 0.123357 | 0.011045 | -0.136397 | -0.010211 |
| -2.12 | -0.155463 | -0.170186 | 0.168389 | -0.052939 | -0.250147 | -0.024656 |

$T_w$. The $\Delta T_w$ values, which were obtained at three instrument temperatures, are less than 0.2 K at most channels and will be used in processing the AMSU-A data. The $w_k$ factor, which equals 1 (0) if the PRT $k$ is determined good (bad) before launch, will be provided for each flight model. Similarly, the mean PRT temperatures of scene and cold targets are defined in the same way as in (2), except without the term $\Delta T_w$.

The T/V calibration data were taken at three instrument temperatures, at each of which, the scene target was sequenced through six temperatures 84, 130, 180, 230, 280, and 330 K, respectively. The cold target was kept at 84 K, but the temperature of the internal blackbody target varies passively from 280 to 300 K, depending on the instrument temperature which is in the range of $-2°$ to 38°C (see Table IV). At each of the scene target temperatures, calibration data were taken for a large number of scans to assure an effective temperature sensitivity less than 0.03 K. The number of scans required depends upon the expected NEΔT of channel 14 (which has the largest NEΔT) and is therefore a function of the scene target temperature. Actual numbers of scans taken at individual temperatures are given in Table I. The uncertainties in knowledge of brightness temperatures and measurement errors [6], which were estimated by the instrument contractor, are listed in Table II.

Antenna beamwidths at all channels were also measured and the values are listed in Table III. One should note that beamwidths at the channels 3–6 and 15 exceed the $3.3° \pm 10\%$ (i.e., $2.97° - 3.63°$) specification. The largest deviation occurs at channel 15 and its measured value is 3.80°. Therefore, the surface resolution will be proportionally larger than the originally specified 48 km at nadir assuming a nominal orbit height of 830 km. Antenna beam efficiency at each channel frequency is 95% (or larger) and the measured values are listed in Table III.

## III. Calibration Algorithm

In this study, radiometric measurements and variables related to the calibration process are given in radiance with dimension of $\mathrm{mW/(m^2\text{-}sr\text{-}cm^{-1})}$, instead of temperature. This is necessary because all other instruments flown on NOAA satellites produce products in radiance. Conversion between brightness temperature and radiance was performed using the full Planck function. The Rayleigh–Jeans approximation is inaccurate as the temperature approaches the space cosmic background temperature 2.73 K, in addition to a frequency-dependent offset [7].

For each scan, the blackbody radiometric counts $C_w$ are the averages of two samples of the internal blackbody. Similarly, the space radiometric counts $C_c$ are the average of two samples of the space target. To reduce noise in the calibrations, the $C_x$ (where $x = w$ or $c$) for each scan line were convoluted over several neighboring scan lines according to a weight function

$$\overline{C_x} = \frac{1}{n+1}\left[\sum_{i=-n}^{n}\left(1 - \frac{|i|}{n+1}\right)C_s(t_i)\right] \tag{3}$$

where $t_i$ (when $i \neq 0$) represents time of the scan lines just before or after the current scan line. The time of the current scan line is $t_0$ and one can write $t_i = t_0 + i\Delta t$, where $\Delta t = 8$ seconds. The $2n+1$ values of $t_i$ are equally distributed about the scan line to be calibrated. Following the AMSU calibration algorithm [5], [8] the value of $n = 3$ is chosen for all AMSU-A antenna systems.

The calibration algorithm developed in [5], which takes into account the nonlinear contributions due to an imperfect square-law detector, convert scene counts to scene radiances. The same calibration algorithm is used in this study to obtain the scene radiance $R_s$, given by

$$R_s = R_w + (R_w - R_c)\left(\frac{C_s - \overline{C_w}}{\overline{C_w} - \overline{C_c}}\right) + Q, \quad \frac{\mathrm{mW}}{\mathrm{m^2\text{-}sr\text{-}cm^{-1}}} \tag{4}$$

where $R_w$ and $R_c$ are the radiances computed from the PRT blackbody temperature $T_w$ and the PRT cold target temperature $T_c$, respectively, using the Planck function. The $C_s$ is the radiometric count from the scene (Earth) target. The averaged blackbody and space counts, $\overline{C_w}$ and $\overline{C_c}$, are defined by (3). The quantity $Q$, which represents the quadratic contribution, is given by [5]

$$Q = u(R_w - R_c)^2\frac{(C_s - \overline{C_w})(C_s - \overline{C_c})}{(\overline{C_w} - \overline{C_c})^2} \tag{5}$$

where $u$ is a free parameter, values of which are determined at three instrument temperatures (low, nominal, and high). The $u$ values at other instrument temperatures will be interpolated from these three values. For channels 9–14 (AMSU-A1-1), two sets of the $u$ parameters are provided; one set is for the primary PLLO#1 and the other one for the secondary PLLO#2.

It should be noted that the ratios in (4) and (5) will eliminate (or reduce) the effect of any channel gain variation on $R_s$. The gain, $G$, of a channel is defined as

$$G = \frac{\overline{C_w} - \overline{C_c}}{R_w - R_c}, \quad \frac{\mathrm{Count}\cdot(\mathrm{m^2\text{-}sr\text{-}cm^{-1}})}{\mathrm{mW}}. \tag{6}$$

The quantity $G$ varies with instrument temperature and remains approximately constant for a fixed instrument temperature. The first two terms in (4) constitute a linear two-point calibration equation, if the quadratic term is negligible. Let $R_{sL}$ denote these two terms

$$R_{sL} = R_w + (R_w - R_c)\left(\frac{C_s - \overline{C_w}}{\overline{C_w} - \overline{C_c}}\right), \quad \frac{\mathrm{mW}}{\mathrm{m^2\text{-}sr\text{-}cm^{-1}}}. \tag{7}$$

We first calculate the radiometric scene radiances $R_{sL}$ from the T/V chamber test data, using this two-point calibration equation. The results are given in Section IV.

## IV. Results

### A. Calibration Accuracy

The "calibration accuracy," $\Delta R$, is defined as the difference between the PRT scene radiance (temperature) and the radiometric scene radiance (brightness temperature) with measured target emissivity of ~0.9999. It is calculated from

$$\Delta R = \frac{1}{N}\sum_{i=1}^{N}(R_{\mathrm{sprt}} - R_{sL})_i \tag{8}$$

where $N$ is the number of scans at individual scene temperatures ($N = 120$ for AMSU-A2 channels but ranging from 400 to 900 for AMSU-A1 channels).

Equation (7) would be a good representation of the microwave radiometric scene radiance from a perfect square-law detector. Any deviation of the quantity $R_{sL}$ from the PRT measured scene radiance $R_{\mathrm{sprt}}$ may indicate the presence of either nonlinearity in the system or some contamination of the calibration data from the T/V chamber. Fig. 1 shows the calculated calibration accuracies versus the PRT scene radiances ($R_{\mathrm{sprt}}$) for channels 1 through 15. The quantities along the ordinates on the left-hand side of these plots represent the calculated $\Delta R$ values from (8), while the corresponding differences in temperature, $\Delta T$ (K), are shown on the right-hand side. The PRT scene temperatures, $T_{\mathrm{sprt}}$, ranging from 84 K (which is also the temperature of the cold target) to

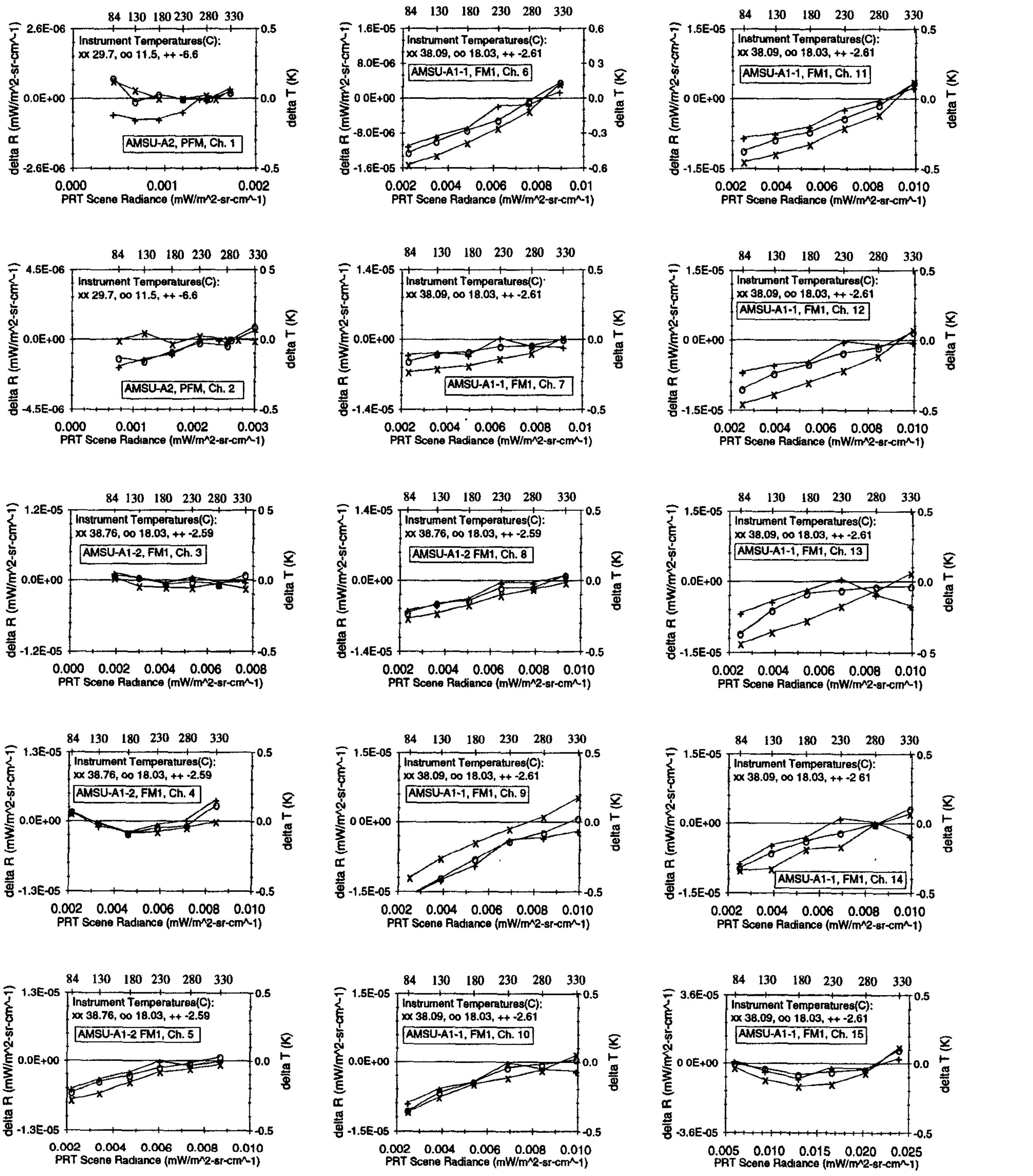


Fig. 1. Calibration accuracies $\Delta R$ versus PRT scene radiances at three instrument temperatures. The corresponding values in brightness temperature $\Delta T$ are labeled at the right-hand sides and the PRT scene temperatures are shown on the top. Note that the patterns of curves at the vertically polarized channels (1–4, 7 and 15) differ from the ones of other channels, which are horizontally polarized.

330 K, are displayed on the upper abscissas. The specification of AMSU-A instruments is required to be $\Delta T \leq 2.0$ K for channels 1, 2, and 15, and $\Delta T \leq 1.5$ K for all other channels. The results in Fig. 1 show that the specifications are met at all channels.

It is interesting to note that the plots in Fig. 1 appear in two different patterns. Those at the channels 1–4, 7, and 15 show little (or very small) $\Delta R$ values at the lower end of the PRT scene radiance (which corresponds to the cold target temperature 84 K), while the remaining channels (5, 6, and 8–14) have relatively large $\Delta R$ values or "cold biases," which can be up to 0.5 K in most channels. The former group of channels all have vertical polarizations (at nadir) and the latter have horizontal polarizations. The magnitudes of these biases are similar to (actually smaller than) those observed in other spaceborne radiometer programs [9]–[10]. The impacts of these calibration errors on the data utility can be estimated from the plots in Fig. 1. Atmospheric brightness temperatures sensed by the channels 5, 6, and 9–14 will be in the range of 200–280 K [9]. The results in Fig. 1 show that the maximum error above 200 K at the nominal instrument temperature, as represented by the open circles, is about 0.2 K; but in most cases, it is less than this as the PRT temperature increases. Most of these errors will be compensated by the nonlinearity corrections, as discussed below. Further discussion of these biases is given in Section V.

### B. Nonlinearity

The residual patterns at channels 4 and 15 (Fig. 1) show clearly the nonlinearity forms which can be represented by the quadratic formula $Q$ defined in (5). Patterns at other channels are not so obvious because of the presence of cold biases. The nonlinearity of a channel is normally obtained from the residuals of a least-squares fit of the PRT scene radiances as a linear function of the radiances RsL. The nonlinearity are obtained from the differences between $R_{\rm sprt}$ and the best-fit results from a linear equation in the form $\text{LinearFit} = a+bR_{\rm sL}$ (where $a$ and $b$ are the intercept and slope). These residuals, which are denoted by $Q = (R_{\rm sprt} - \text{LinearFit})$, are shown in Fig. 2. The largest (absolute) $Q$ value on each curve is defined as its nonlinearity.

The plots in Fig. 2 show the measured nonlinearities between 84 and 330 K. One can see that the maximum (absolute) $Q$ values are about 0.1 K, which can be observed at channels 1, 4, 6, 9, 10, 11, 13, 14, and 15, respectively. The AMSU-A specification is required to have $Q \leq 0.5$ K for channels 1, 2, and 15; and $Q \leq 0.375$ K for other channels. The results in Fig. 2 show that the specifications are met at all channels.

Most of the curves in Fig. 2 have two roots and can be easily fitted by a quadratic equation, which can be written in the form

$$Q = u(R_s - R_1)(R_s - R_2) \qquad (9)$$

where $R_1$ and $R_2$ represent the two roots. One can obtain a similar equation from (5) by replacing the counts by its individual radiances, since the radiometric counts are proportional to radiances in a first-order approximation. The resultant equation represents a different straight line intersecting the same curve at $R_w$ and $R_c$ (corresponding to the internal blackbody temperature $T_w$ and the cold target temperature $T_c = 84$ K, respectively). Once the parameter $u$ is determined, it can be used with any pair of roots to calculate $Q$. In the case of in-orbit data, the two roots will be located at $T_c = 2.73$ K and $T_w = 300$ K, respectively. We applied (9) to fit the quadratic curves in Fig. 2 and obtained the $u$ values (with the two roots extracted from each plot). Table IV gives the best-fit $u$ values at three instrument temperatures, at which the cycles of data were collected. The $u$ values for channels 9–14 were obtained for both PLLO#1 and PLLO#2.

### C. Simulation of Quadratic Corrections to Space Data

Once the $u$ values are determined, (9) can be used to simulate the nonlinearities between 2.73 and 300 K, which is the range of in-orbit data. This can be accomplished by replacing the roots $R_1$ and $R_2$ with the radiances $R_{2.73}$ and $R_w$ (corresponding to $T_c = 2.73$ K and $T_w = 300$ K, respectively) and (9) becomes

$$Q = u(R_s - R_{2.73})(R_s - R_w). \qquad (10)$$

The simulated $Q$ values from (10) are shown in Fig. 3 for all channels at three instrument temperatures. These simulated nonlinearity curves have $Q = 0$ at the calibration reference points corresponding to $T_c = 2.73$ K and $T_w$, but the plots in Fig. 3 stop at 84 K, below which there are no data. One should note the differences between the results shown in Figs. 2 and 3. This is expected because the factor $(R_s–R_{2.73})$ in (10) is much larger than the corresponding one in (9). Fig. 3 shows that there are little nonlinearities at channels 5 and 8 and that a very small magnitude of contribution (~0.02 K) appears in channel 3. Noticeable quadratic contributions appear at other channels. The largest one occurs at channel 15 and has a magnitude of 0.3 K at the high instrument temperature 38.09°C. Also, channels 4, 6, 10, 11, 12, 13, and 14 have nonlinearities with magnitude between 0.1 and 0.2 K, while the remaining ones are less than 0.1 K.

### D. Temperature Sensitivity

The temperature sensitivity (or NEΔT) requirements for AMSU-A channels are listed in Table III. It is defined as the minimum change of scene brightness temperature that can be detected. In practice, it is calculated as the standard deviation of the radiometer output (in K), when an antenna system is viewing a scene target at 300 K. These calculated NEΔT values (see Table III) correspond to a scene temperature of 305 K, because they are the mean values of two measurements taken at the scene target temperatures of 280 K and 330 K, respectively (no calibration data were taken at 300 K).

## V. Conclusion and Discussion

We have analyzed the T/V chamber calibration data from the AMSU-A2 PFM and AMSU-A1 FM1, both of which will be flown on NOAA-K. The results show that both models meet the instrument specification in calibration accuracy, nonlinearity, and temperature sensitivity. However, the 3-dB antenna beamwidths at the AMSU-A1 channels slightly exceed the specification limits of 3.3° ± 10%.

The existence of nonlinearity is shown in most of the channels. We developed a quadratic formula for modeling these nonlinear contributions, which were characterized by a single parameter $u$. The $u$ values at three instrument temperatures were obtained for individual channels using a least-square fit method. Using the best-fit $u$ values, we performed a series of simulations of the quadratic corrections which would be expected from in-orbit data after the launch of AMSU-A on NOAA-K. In the simulations, the cold space radiance

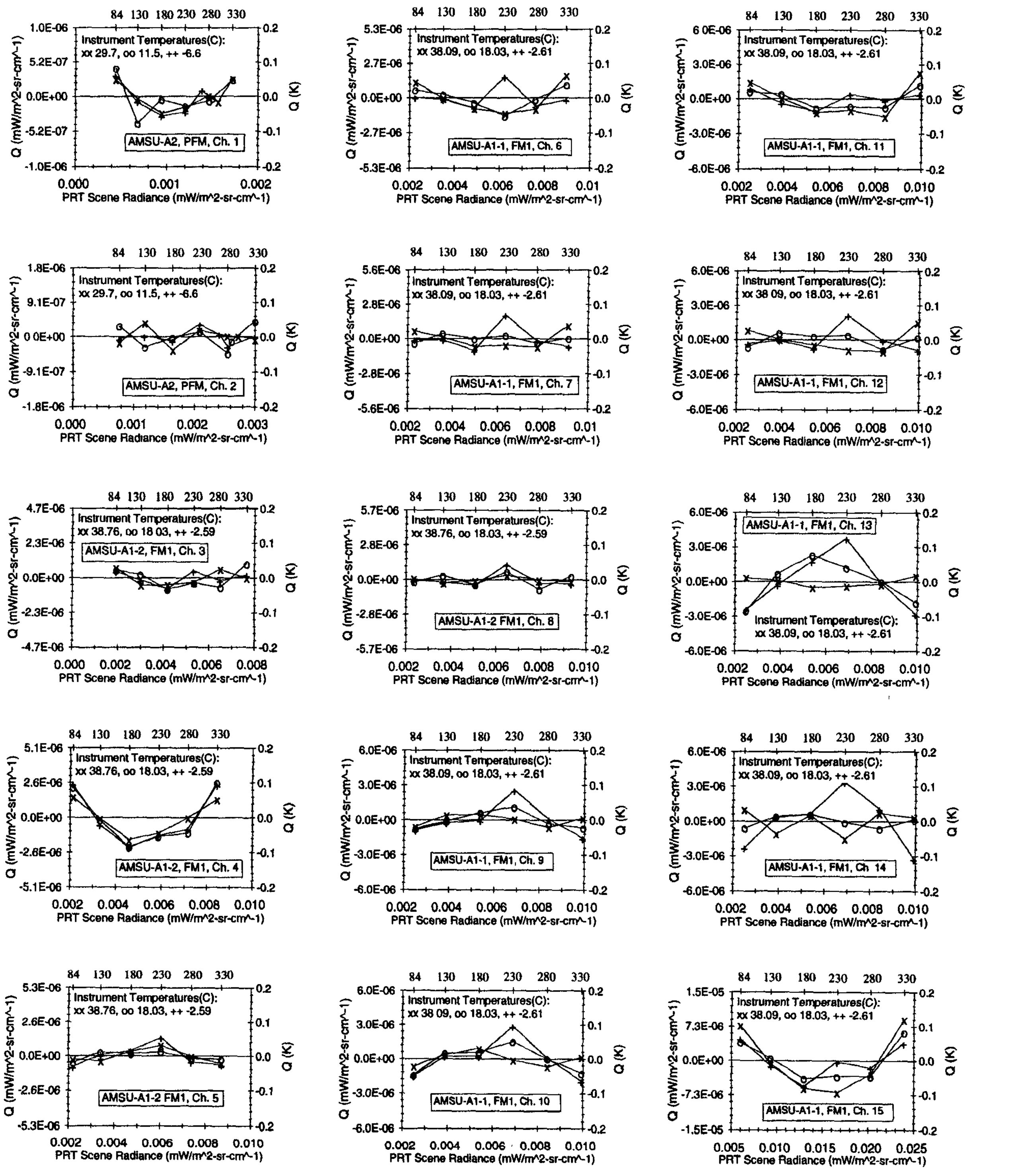


Fig. 2. Measured nonlinearities between 84 and 330 K. The largest (absolute) $Q$ value on each curve is defined as the measured nonlinearity. The specifications are required to be $Q \leq 0.5$ K for channels 1, 2, and 15, and $Q \leq 0.375$ K for other channels.

corresponding to the cosmic background temperature 2.73 K was adopted as one of the two reference calibration points (the other reference point is at the internal blackbody temperature $T_w$). The largest nonlinear correction is about 0.3 K, which occurs at channel 15 when the instrument temperature is at 38.09°C. Others are less than 0.2 K.

In general, the qualities of the T/V chamber test data from both AMSU-A2 PFM and AMSU-A1 FM1 are quite good. Particularly, the instrument temperatures were all stabilized at preselected values with total variation less than ±0.5 K during each test cycle. This renders the measured instrument nonlinearities more reliable and the results from this study confirm the high quality of the AMSU-A instruments for NOAA-K.

It was found that the calibration accuracies are polarization-dependent. Channels with vertical polarizations show little

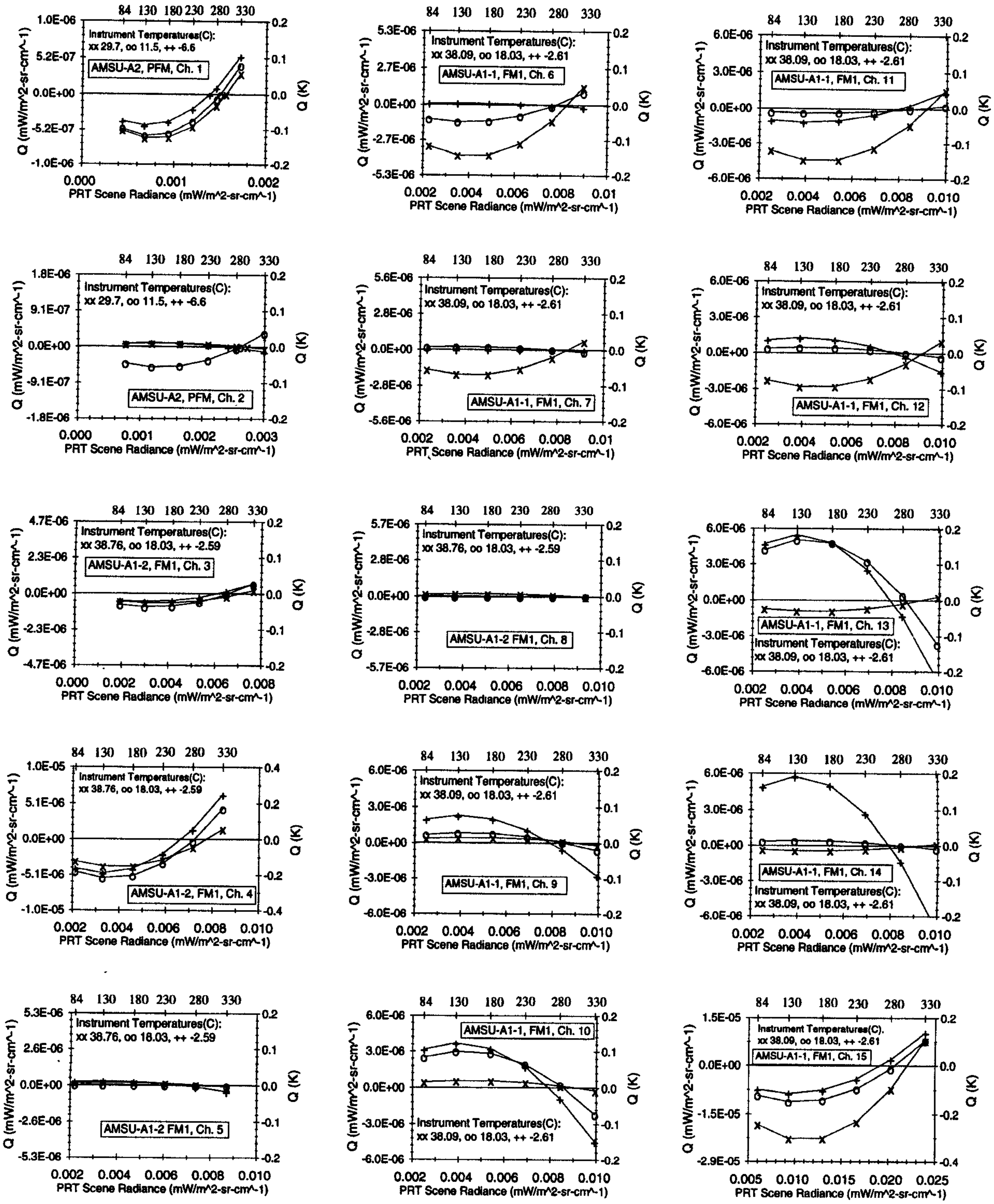


Fig. 3. Simulated nonlinearities from (10). These would be expected from in-orbit data after the launch of AMSU-A on NOAA-K.

cold biases at the cold and scene target temperature 84 K, while those with horizontal polarizations all have appreciable cold biases, which can be up to 0.6 K. This polarization dependence of the calibration accuracy is an interesting but peculiar phenomena of the calibration data. At the present time, it is not well understood how these polarization-dependent cold biases originate. However, there are some trends which may provide us with some clues. The cold biases from channels with horizontal polarization are all negative. This implies [see (8)] that excess radiances are received in the horizontally polarized channels. These excess radiance is polarization-dependent, therefore, it can not be due to thermal energy from the T/V chamber surroundings or sidelobe contamination, both of which would affect the two polarizations equally. Also, the effect can not be attributed to a target defect or PRT temperature anomaly since both vertically and horizontally polarized channels share same targets. Based on these facts, the AMSU-A manufacturer suggests that a likely source for the observed cold biases is due to some low-level coherent microwave radiation leakage from the instrument itself. Such type of energy would be polarization sensitive and it has a larger effect at cooler target temperatures, where the ratio of leakage power to that of radiometer is larger [6]. From a scientific point of view, it is highly desirable to find the source of the biases, but it would require a major effort by the instrument builder to accomplish this.

Comparing to the currently operational Microwave Sounding Unit (MSU) on the NOAA POES [9], the new AMSU-A instruments will provide greatly improved accuracy in retrievals of atmospheric temperature profiles. In accompanying each AMSU-A, there is also an AMSU-B, which has 5 channels with frequencies at 89, 150, and 183–190 GHz [10]. AMSU-B, which is provided by the U. K. Meteorological Office, is for humidity sounding and has been described elsewhere [10]. The results presented in this study should be useful to those who want to understand the AMSU-A data.

## Appendix A
## System Description of AMSU-A

The detailed description of AMSU-A system can be found in various Aerojet s reports and only a brief summary (taken from these reports) is given in this appendix. The basic operation of AMSU-A1 and -A2 modules is very similar. Each module is configured in the same fashion, and consists of antenna, electronics (receiver and signal processor), mechanical, and thermal assemblies.

The cross-track scanning of the antenna system is accomplished in a stepped fashion with a dwell of 165 msec for AMSU-A1 and 158 msec for AMSU-A2 at each of the 30 Earth viewing positions and a 370-msec dwell at the cold and warm calibration positions, where two samples are collected, respectively. Stepping of the antenna is accomplished in a rapid-step fashion and a complete revolution of the antenna is completed in 8 seconds. Each antenna system is configured with a shrouded parabolic reflector assembly that is fed with a wideband conical horn to provide a high-efficiency beam. A closed-path calibration system provides a guided path to the calibration source without introducing extraneous signals. The radiometer is calibrated every 8 seconds by viewing a blackbody target at ~290 K and the 3 K comic background radiation (in the T/V chamber test, the latter was simulated by a 84 K cold target).

Each receiver is a total power, superheterodyne configuration that uses a combination of Gunn diode cavity-stabilized and phase-locked loop, crystal derived oscillators to provide channel frequency stability. Following RF, the mixers and oscillators translate RF frequencies to intermediate frequencies (IF). Predetection gain and passband characteristics are achieved by low-noise IF amplifiers and bandpass filters. Channel center frequency stabilization is provided by invar cavity stabilization of the Gunn diode oscillators. A Gunn oscillator phase-locked to the harmonic of a crystal provides the frequency stability required in Channels 9 through 14. Square law detectors convert receiver output power to a dc voltage equivalent of temperature. The signal is further amplified in video amplifiers and integrate-and-dump (ID) filters. The A/D convertor digitizes the ID filter outputs. A microcomputer transfers data from the A/D convertor to the spacecraft.

## Appendix B
## Polynomial Coefficients for Converting PRT Counts into Temperatures

The two-step process for deriving the PRT temperatures from PRT counts $C_k$ is briefly described here. First the $C_k$ from each PRT is converted into to resistance $r_t$ (in ohms) by a polynomial

$$r_t = \sum_{i=0}^{3} A_i C_k^i \tag{B1}$$

where the coefficients $A_i$ for individual PRT's and temperature sensors were provided by Aerojet. Once the resistance $r_t$ is known, one can calculate the PRT temperature $t$ (in Celsius) from the Van Dusen equation [3], which is given by

$$\frac{r_t}{r_o} = 1 + \alpha\left[t - \delta\left(\frac{t}{100} - 1\right)\left(\frac{t}{100}\right) - \beta\left(\frac{t}{100} - 1\right)\left(\frac{t}{100}\right)^3\right] \tag{B2}$$

where

$r_t =$ resistance (in ohms) at temperature $t$ (°C) of the blackbody target

$r_o =$ resistance at $t = 0$°C (supplied by the manufacturer via Aerojet)

$\beta = 0$ for $t > 0$°C, and 0.11 for $t < 0$°

$\alpha$ and $\delta$ are constants provided by the manufacturer.

Calculation shows that the error is negligible by setting $\beta = 0$ in (B2). In such case, one can solve the quadratic equation for $t$ in terms of $r_t$. Then the PRT temperature in degree Kelvin is obtained from $t + 273.15$. By this way, datasets of PRT temperatures as a function of counts for individual PRT's are computed. Then (1) is applied to fit these datasets for obtaining the polynomial coefficients $f_{kj}$ for individual PRT's and housekeeping sensors. Test calculations show that these polynomials are highly accurate (with errors in the order of 0.001 K) in reproducing temperatures of PRT's and sensors.

## Acknowledgment

The author would like to thank R. Legeckis for allowing use of the VAX computer at the Oceanic Sciences Branch where the computations and processing of the calibration data were done. Also thanks to D. Wark for his valuable advice and continued support in the AMSU-A project and to J. P. Green of NOAA/SPO and S. Krimchansky of NASA/GSFC for their management of the AMSU-A Program. Aerojet is the primary AMSU-A contractor for building the instruments and its test reports provided us with valuable information.

## REFERENCES

[1] "Delta CDR for the advanced microwave sounding unit-A," Aug. 1991, Aerojet, Azusa, CA 91702.
[2] P. K. Patel and J. Mentall, "The advanced microwave sounding unit-A (AMSU-A)," *Microwave Instrumentation for Remote Sensing of the Earth*, SPIE, vol. 1935, Orlando, Apr. 13–14, 1993, pp. 130–135.
[3] *PRT Handbook*, Bulletin 1042, 1986, Rosemount Inc., Burnsville, MN 55337.
[4] The NOAA anonymous ftp address is: sdsd.nesdis.noaa.gov, user ID: ftp, password: your email address, and directory: /pub/doc/. Information for new users is in files INDEX and KLMREAD.ASC.
[5] T. Mo, M. Weinreb, N. Grody, and D. Wark, "AMSU-A engineering model calibration," NOAA Tech. Rep. NESDIS 68, 1993.
[6] Aerojet, Azusa, CA, private communication, 1996.
[7] M. A. Janssen, "An introduction to the passive microwave remote sensing of atmospheres," in *Atmospheric Remote Sensing By Microwave Radiometry*. New York: Wiley, ch. 1, 1993.
[8] D. Wark *et al.*, "NOAA-KLM data processing specifications," NOAA/NESDIS internal memorandum, 1994.
[9] T. Mo, "A study of the microwave sounding unit on the NOAA-12 satellite," *IEEE Trans. Geosci. Remote Sensing*, vol. 33, pp. 1141–1152, 1995.
[10] R. W. Saunders, T. J. Hewison, N. C. Atkinson, and S. J. Stringer, "The radiometric characterization of AMSU-B," *IEEE Trans. Microwave Theory Tech.*, vol. 43, pp. 760–771, 1995.

**Tsan Mo** received the Ph.D. degree in physics from the University of Maryland.

He worked in the fields of nuclear physics, atmospheric sciences, and microwave remote sensing. Currently, he is employed at the NOAA/NESDIS Satellite Research Laboratory and works on the advanced microwave sounding unit-A, which will be launched on the NOAA polar-orbiting environmental satellites during the next decade.